

## THEORY AND TECHNOLOGY OF FORMING PROCESS

### FORMATION AND PROPAGATION OF SHOCK WAVES IN HIGHLY POROUS MATERIALS

M. B. Shtern<sup>1,2</sup> and E. V. Kartuzov<sup>1</sup>

UDC 621.762.96

*The existence issue of shock waves during dynamic deformation of plastic porous materials is analyzed. The analysis is based on the mechanics of plasticity for porous continuum. The deformation routes typical for both the use of shock resistant materials and dynamic compaction of powders and porous bodies are considered. It is established, that unlike compacts, the deformation of porous bodies can be accompanied by shock waves. For the routes where the changes in volume dominate over the changes in shape, the deformation is always accompanied by the formation of shock waves. Meanwhile, in case of free deposition (and similar routes), shock waves appear only if the starting porosity is high.*

**Keywords:** shock wave, high porosity materials, dynamic loading.

#### INTRODUCTION

Various aspects of the behavior of new materials under high-rate loading are traditionally in the focus of experts in the field of the formation and operation of materials. In accordance with the above, the problems of dynamic effects on materials can be divided into two main groups. *The first group* is the application of dynamic methods to form a structure capable of ensuring the desired properties. *The second group* is the design of products containing the elements that provide resistance to the shock loads and resulting effects [1]. The processes based on the dynamic impact are widespread in powder metallurgy (PM) [2]. The need for their improvement contributed to the development of theoretical concepts of this process [3]. Meanwhile, a number of issues related to the use of high strain-rate compaction remains unsettled due to the lack of understanding of the wave reaction of material on the high rate irreversible deformation.

Materials science of shock-resistant materials benefits a significantly increased interest in recent decades. One of the main directions of this research is the design of products, whose internal structure is able to minimize the effects of the shock pulse. In this regard, the scientists paid special attention to the highly porous materials. However, creating a structure that promotes absorbing of the shock pulse required to deepen the understanding of the dynamic response of such materials.

<sup>1</sup>Frantsevich Institute for Problems of Materials Science, National Academy of Sciences of Ukraine, Kiev, Ukraine.

<sup>2</sup>To whom correspondence should be addressed; e-mail: mbsh07@ukr.net.

---

Translated from Poroshkovaya Metallurgiya, Vol. 55, No. 3–4 (508), pp. 13–22, 2015. Original article submitted February 8, 2016.

The understanding of the pulse propagation in porous solids is common to the above areas of materials science. The features of formation and propagation of the shock waves resulting from the loading pulse acquire a special importance. In relation to PM processes, this issue was addressed in [2, 4, 5]. The studies have established that shock waves may form and propagate during powder compaction in rigid dies. A large number of studies are devoted to the behavior of highly porous materials under high rate deformation, where the existence of shock waves in porous bodies is also considered in details [6–8]. In particular, the authors [8] have experimentally established the dependence of the shock wave existence and the structure of the shock front on the internal geometry of the cellular body and the kinematic restrictions applied to the loaded cylindrical sample of foamed aluminum.

Analysis of this and other studies on the propagation of the shock waves in porous and powder materials indicates a significant dependence of the shock front formation conditions and its evolution during dynamic loading on the porous structure. However, the questions: “What are the deformation routes the shock waves may exist at?” and “How the starting porosity and possible kinematic restrictions affect this?” remain unanswered.

The purpose of this study is to establish the features of formation and propagation of shock waves in highly porous materials, using the mechanics of plasticity for porous continuum.

### PLANE SHOCK WAVES AND THEIR FORMATION

According to the concepts of continuum mechanics [6, 9, 10], the shock wave is a surface, which moves inside the loaded body and meets the following condition: when going through this surface, the density, the normal components of the velocity vectors and strains, and the temperature undergo discontinuous changes. In this study, we are limited to the assumption that such surface is flat and is formed as a result of the impact of a solid non-deformable object, limited by a flat surface on one of the ends of the cylinder, perpendicular to its axis (Fig. 1). The moving surface is called a plane shock wave, generated by a pulsed stress  $\sigma_z$  applied to an end face of the cylinder.

The formation of the shock wave is determined by the following factors. It is known that, as a result of the pulsed loading (Fig. 1), density  $\rho$ , stress  $\sigma_z$ , and axial displacement are in the relationship reflecting Newton’s second law:

$$\rho \frac{\partial^2 u_z}{\partial t^2} = \frac{\partial^2 \sigma_z}{\partial z^2}, \quad (1)$$

where  $u_z$  is the shear vector,  $t$  is the time. It is assumed that  $\sigma_z$  is the function of the axial component of the low-strain tensor  $\partial u_z / \partial z$ :  $\sigma_z = f(\partial u_z / \partial z)$ . Substituting this relationship in (1), we obtain the equation describing the propagation of small perturbations along the axis  $z$  inside the cylinder examined:

$$\rho \frac{\partial^2 u_z}{\partial t^2} = f' \left( \frac{\partial u_z}{\partial z} \right) \frac{\partial^2 u_z}{\partial z^2}. \quad (2)$$

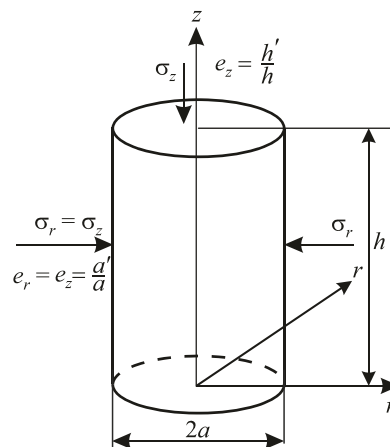


Fig. 1. Deformation rates  $e_r$ ,  $e_z$  and stresses  $\sigma_r$ ,  $\sigma_z$ , resulting of the axial dynamic loading of the cylinder in the direction opposite to the axis  $z$

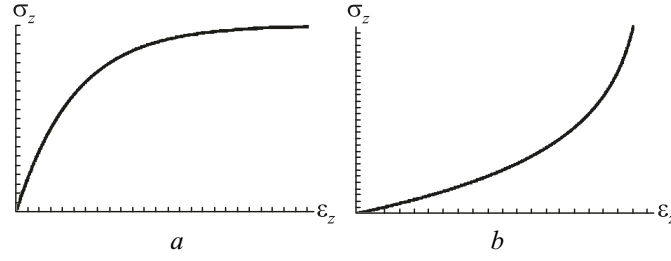


Fig. 2. Relationship between  $\partial u_z/\partial z$  and  $\sigma_z$ : convex (a) and concave (b)

The propagation of small perturbations can be identified by referring to the derivative of the function  $f(\partial u_z/\partial z)$ , the square root of which is equal to the speed of their propagation. The convex function (Fig. 2a) indicates a decrease in the rate of small perturbations. As a result, the perturbation amplitude is not increasing and the velocity of the axial movement and the axial stress remain continuous functions of  $z$ .

The concave function (Fig. 2b) indicates an increase in the rate of small perturbations: the perturbations generated at the later stages catch up those generated at the earlier stages of the process. Herewith, the amplitude of the propagation front of perturbations increases dramatically. Subsequently, the velocity of the axial movement and the axial stress undergo a discontinuous change, when passing this front. The Rankine–Hugoniot relations [8–10] display, that the density also undergoes a jump (compression shock), when passing this front. According to Euler, the value  $\partial u_z/\partial z$  can be identified with the axial strain  $\varepsilon_z$  within the adopted schemes. Therefore, the existence of the shock wave is conditioned by the concave curve “ $\sigma_z-\varepsilon_z$ ”. The curve “ $\sigma_z-\varepsilon_z$ ” is not concave during plastic deformation of materials that contain no pores and prevent irreversible changes in volume (for example, reinforcing materials that satisfy the von Mises plasticity model).

#### CONSTITUTIVE EQUATIONS FOR PLASTIC POROUS BODIES

The existence of shock waves in porous materials can be determined using the theory of plasticity for porous bodies that takes into account the entire range of changes in porosity. In one of the most cited studies on cellular body deformation [11] the theory of plasticity, in which the loaded surface is assumed in the form of an ellipse in the “average stress–stress deviator intensity” space, was applied. This exact model was previously developed in Frantsevich Institute for Problems of Materials Science, NAS of Ukraine [12–15]. In this study, it is presented by the following equations:

$$\sigma_z = \varphi \frac{\sigma_0}{W} \left( \frac{1-\nu}{1-2\nu} e_z + 2 \frac{\nu}{1-\nu} e_r \right), \quad (3)$$

$$\sigma_r = \varphi \frac{\sigma_0}{W} \left( \frac{\nu}{1-\nu} e_z + \frac{1}{1-2\nu} e_r \right), \quad (4)$$

$$W = \frac{\sqrt{\varphi}}{\sqrt{(1-\theta)(1-2\nu)}} \sqrt{2e_r^2 + 4\nu e_r e_z + (1-\nu)e_z^2}, \quad (5)$$

where  $W$  is the equivalent strain rate,  $\theta$  is the porosity,  $\varphi = (1-\theta)^2$ , and  $\nu = (2-3\theta)/(4-3\theta)$ .

Note that  $\varphi$  characterizes the shear properties, while  $\nu$  characterizes the lateral contraction factor (analog of Poisson’s ratio for plastically compressible media). Both parameters have been introduced by Skorokhod [16] based on the micromechanical analysis. Their characterization guarantees that a full range of changes in the porosity (from 0 to 1) is considered. In particular, such characterization for  $\nu$  is justified by the fact that the requirement  $-1 \leq \nu \leq 1/2$  is satisfied just in this range.

The parameter  $\sigma_0$  is the yield stress of the material at  $\theta = 0$ , multiplied by  $\sqrt{2/3}$ . Since the dimensionless stress will be analyzed below and the strain hardening of the base material of porous body is not considered, the numerical value of this parameter can be chosen arbitrarily. To present the study results in a more visible manner, the effects of reinforcing the porous body matrix were ignored. This issue has been addressed in [5].

Deleting  $e_r$ ,  $e_z$ , and  $W$  from Eqs. (3)–(5), we obtain the equation of the loaded surface, which (in the symbols changed) corresponds to the reasoning in [12–15]:

$$3 \frac{(1-2\nu)}{1+\nu} p^2 + \tau^2 = (1-\theta)\phi\sigma_0^2, \quad (6)$$

where  $p = 1/3(\sigma_z + 2\sigma_r)$ ,  $\tau = \sqrt{2/3}|\sigma_z - \sigma_r|$ .

### STRESS-STRAIN RELATIONSHIP FOR DEFORMATION, UNIAXIAL LOADING, AND CONSTRAINED SIDEWALL DEFORMATION

In this study, we can neglect the factors contributing to an uneven distribution of stresses and porosity inside the samples, in particular, the effect of the external friction. Let us consider the uniaxial deformation of porous bodies in which all components (except the axial one) of the strain rate tensor equal zero. PM identifies this process as compression in the mold (Fig. 3a).

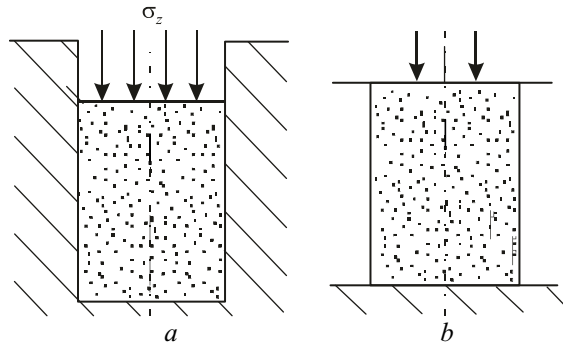


Fig. 3. Uniaxial deformation (a) and loading (b)

In this case, Eqs. (3)–(5) are simplified significantly and the equation for the uniaxial stress reads as follows:

$$\sigma_z = \sigma_0 \sqrt{\frac{(1-\theta)(1-\nu)}{1-2\nu}} \phi. \quad (7)$$

Meanwhile, this equation describes the dependence of the axial pressure on the porosity, but not on the strain. Therefore, it should be supplemented by the equation correlating the porosity and strain. In the absence of the velocity radial component, this equation derives from the law of conservation of mass, where the relationship between the porosity and density is considered as  $\rho = \rho_m(1-\theta)$ :

$$\varepsilon_z = \ln\left(\frac{1-\theta_0}{1-\theta}\right), \quad (8)$$

where  $\rho_m$  is the density of the porous body matrix material,  $\theta_0$  is the starting porosity.

During uniaxial loading (Fig. 3b), it is assumed that all components (except the axial one) of the strain rate tensor equal zero. Then, it follows from Eqs. (3)–(5):

$$\sigma_z = \sigma_0 \sqrt{\phi(1+\nu)(1-\theta)}. \quad (9)$$

The axial deformation was determined with allowance for the assumption  $\sigma_r = 0$ . Then, it follows from Eq. (4):

$$e_r = -\nu e_z. \quad (10)$$

With allowance for Eq. (10) in the law of conservation of mass, which correlates the change in porosity in time with the strain rate tensor components by Eq. (11), we come to the differential equation (12):

$$\frac{d\theta}{dt} = (1-\theta)(e_z + 2e_r), \quad (11)$$

$$\frac{d\theta}{dt} = (1 - \theta)(1 - 2\nu)e_z. \quad (12)$$

Since a logarithmic measure of the strain is used, the equation for  $e_z$  can be obtained from Eq. (12) and expressed as follows:

$$\varepsilon_z = \frac{1}{3} \left( \ln \left( \frac{-1 + \theta}{-1 + \theta_0} \right) - 4 \ln \left( \frac{\theta}{\theta_0} \right) \right). \quad (13)$$

The uniaxial loading under the constrained sidewall deformation takes an intermediate position between the two discussed above. Let us suppose that the cylindrical sample is enclosed in a cylindrical cavity retainer that allows the radial movements in the direction from the cylinder axis, but restricts them. To make allowance for this restriction a compliance of the cavity retainer  $k$  (which make it possible to convert the ratio between the radial and axial strain rate components into  $e_r = -kve_z$ ) was introduced. This assumes that  $k$  satisfies the inequality  $0 \leq k \leq 1$ . In the case of uniaxial deformation, the last equality leads to  $e_r = 0$ . In the case of uniaxial loading ( $\sigma_r = 0$ ), Eq. (10) holds.

The calculations (similar to those conducted for uniaxial loading) are represented by the following Eqs. for the axial stress and axial strain:

$$\sigma_z = \sqrt{\frac{2(-1 + \theta)^3(-4 + k(2 - 3\theta)^2 + 3\theta)^2}{3(4 + (-2 + k)k(2 - 3\theta)^2 - 3\theta)\theta(-4 + 3\theta)}} \sigma_0, \quad (14)$$

$$\varepsilon_z = \frac{-\ln\left(\frac{-1 + \theta}{-1 + \theta_0}\right) - 2k \ln\left(\frac{-1 + \theta}{-1 + \theta_0}\right) + 4k \ln\left(\frac{4 - 4k - 3\theta + 6k\theta}{4 - 4k - 3\theta_0 + 6k\theta_0}\right)}{-1 + 4k^2}. \quad (15)$$

#### ANALYZING THE CONVEXITY OF STRESS–STRAIN CURVES

Performing simple mathematical procedures to exclude the porosity of the three equation pairs above for axial stresses and axial strains, we can obtain the graphical representations of the relationships between these values. All further diagrams were obtained for different values of starting porosity in the 0.2–0.9 range.

Irrespective of the starting porosity, all curves are concave (Fig. 4) during uniaxial deformation. However, this fact is quite expected, because the compaction and second compaction of porous bodies clearly demonstrate that the curve of the axial stress (during compression in the mold) has an asymptote. This asymptote is better known from the pressure–density relationship and is connected with the fact that the density of the material particles cannot be exceeded in the pressure operating range, typical for PM. However, the situation is different during uniaxial loading (Fig. 4b). When  $\theta < 0.5$ , the stress–strain curves are close to those that are well-known from the mechanics

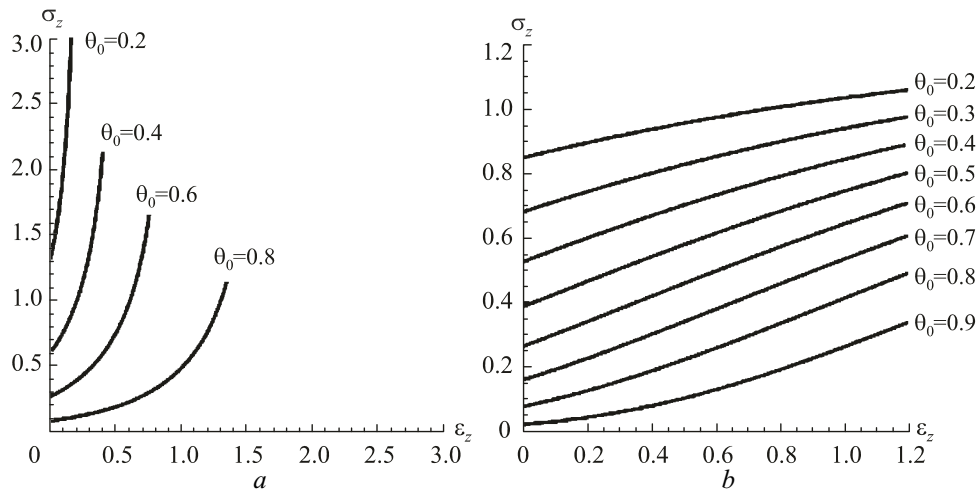


Fig. 4. Variation “axial stress–axial strain” during uniaxial deformation (a) and loading (b)

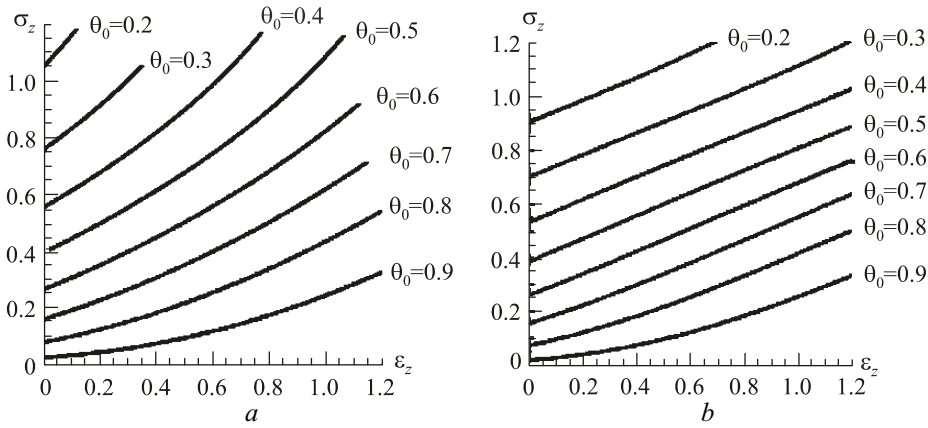


Fig. 5. Variation of “axial stress–axial strain” during uniaxial loading with constrained sidewall deformation conditions:  $k = 0.8$  (a) and  $0.9$  (b)

of strained compact metals: the curves are convex. With increasing the starting porosity, a noticeable flattening of the curves is observed. When  $\theta_0 \geq 0.8$ , the relationship changes: the curve is concave, as in the case of uniaxial deformation. However, unlike uniaxial deformation, no signs of vertical asymptote are observed (Fig. 4b) during uniaxial loading.

In the case of uniaxial loading with constrained sidewall deformation, the behavior of curves is determined not only by the starting porosity, but also by the compliance  $k$ . When  $k = 0.8$ , the behavior of stress–strain curves is very close to that of the curves during uniaxial deformation (Fig. 5a). Only when  $k = 0.9$ , the behavior of the curves becomes similar to uniaxial loading.

### THE FORMATION OF SHOCK WAVES

Based on the analysis of stress–strain dependency, the conditions of the formation of plane shock waves during dynamic impact on porous body in a wide range of changes in  $\theta_0$  have been established. Unlike strained non-compressible metals governed by the von Mises plasticity model and the most common reinforcement conditions, porous bodies allow a range of compression and loading routes that shock waves can form under. For example, the uniaxial deformation (Fig. 4) and uniaxial loading with kinematic restrictions (Fig. 5). Primarily, these are the routes with a dominating hydrostatic component of the stress state. As a rule, a kinematic restriction on forming occurs in such situation, resulting in the asymptote in the stress–strain relationship and a corresponding concave curve. Both loading routes and mechanisms for the formation of shock waves are quite similar to the phenomena accompanying the compression of ideal gases by a plunger in a closed vessel. The analogy between this process and uniaxial deformation of porous bodies is based on the similarity of pressure–density relationships, which in both cases are characterized by concave curves.

Unlike uniaxial deformation, during uniaxial loading, the behavior of porous body with low porosity is analogous to that of the compact materials and shock waves cannot occur [10]. However, with the starting porosity of  $\approx 1$ , the curves are concave (Fig. 4b) and thus, the formation of shock waves becomes the expected.

Apparently, the reason of the specified anomaly can be found in the equation for the lateral contraction factor, which becomes negative for such high porosity values [16, 17]. In this case, in the initial stages of compression, the radial flow rate of the porous sample is directed towards the cylinder axis, hereupon, the behavior of the sample is similar to a hydrostatic compression. While compacting, the flow behavior approaches that typical for the uniaxial deformation. This may cause the formation of the concave curve and, hence, the formation of shock waves.

It should be noted that the results of the proposed analysis are based on several hypotheses that simplify calculations. For example, the porosity is the only material parameter in this study. It is promising to supplement the material model with other structure parameters that can be used for explaining and controlling the dynamic deformation of porous bodies.

## CONCLUSIONS

All porous materials are able to irreversibly change the volume during plastic deformation. The compression and loading routes, when the curves of the stress–strain relationship are concave, are feasible exactly for the porous materials. The compression in the absence or a significant restriction of the velocity component perpendicular to the impact direction comes first among these routes. Under these conditions, a plane shock wave forms in the volume of the sample.

Easing restrictions may demonstrate the transformation of the shock wave into the plane compressive wave followed by its suppression. If the application of the impact load complies with the uniaxial loading route (free settlement), the formation of shock waves is typical only for the initial stage of the process, provided that the starting porosity is  $\approx 1$ . In this case, however, with increasing deformation, a transformation of the shock wave into the compressive wave occurs, accompanied by a sharp decrease in its amplitude.

## REFERENCES

1. M. A. Mayers, *Shock Waves and High Strain-Rate Phenomena in Metals* [Russian Translation], Metallurgiya, Moscow (1984), p. 512.
2. Yu. G. Dorofeev, *Dynamic Isostatic Pressing of Cermets* [in Russian], Metallurgiya, Moscow (1972).
3. O. V. Roman and V. G. Gorobtsov, *Pulsed Loading of Powder Materials in: Actual Problems in Powder Metallurgy* [in Russian], O. V. Roman and V. S. Arunachalama (Eds.), Metallurgiya, Moscow (1990), pp. 78–99.
4. L. A. Maksimenko, A. L. Maksimenko, G. G. Serdyuk, and M. B. Shtern, “Shock waves in dynamic powder and porous-body compaction. Part I. Local features of powder compaction in rigid dies,” *Powder Metall. Met. Ceram.*, **30**, No. 7, 553–556 (1991).
5. L. A. Maksimenko, A. L. Maksimenko, G. G. Serdyuk, and M. B. Shtern, “Shock waves in dynamic compacting powders and porous bodies. Part II. Propagation of shock waves in porous materials with a reinforcing frame,” *Powder Metall. Met. Ceram.*, **30**, No. 9, 726–729 (1991).
6. Ya. B. Zel’dovich and Yu. P. Raizer, *Physics of Shock Waves and High-Temperature Hydrodynamic Phenomena* [in Russian], 2-nd edition, Nauka, Moscow (1966), p. 688.
7. L. J. Gibson and M. F. Ashby, *Cellular Solids: Structure and Properties*, 2-nd edition, Cambridge University Press, Cambridge, UK (1997), p. 532.
8. D. D. Radford, V. S. Deshpande, and N. A. Fleck, “The use of metal foam projectiles to simulate shock loading on a structure,” *Int. J. Impact Eng.*, **31**, 1152–1171 (2005).
9. R. Courant and K. O. Friedrichs, *Supersonic Flow and Shock Waves*, Springer-Verlag, New York (1948), p. 464.
10. V. K. Novatskii, *Wave Challenges in the Theory of Plasticity* [in Russian], Mir, Moscow (1978), p. 307.
11. V. S. Deshpande and N. A. Fleck, “Isotropic constitutive models for metallic foams,” *J. Mechan. Phys. Sol.*, **48**, 1253–1283 (2000).
12. V. V. Skorokhod, M. B. Shtern, and I. F. Martynova, “Theory of nonlinearly viscous and plastic behavior of porous materials,” *Powder Metall. Met. Ceram.*, **26**, No. 8, 621–626 (1987).
13. M. B. Shtern, “Development of the theory of pressing and plastic deformation of powder materials,” *Powder Metall. Met. Ceram.*, **31**, No. 9, 735–745 (1992).
14. M. B. Shtern, G. G. Serdyuk, L. A. Maksimenko, et al., *Phenomenological Theories of Powder Pressing* [in Russian], Naukova Dumka, Kiev (1982), p. 140.
15. M. B. Shtern and B. D. Rud’, *Mechanical and Computer Models for Consolidating Granular Media* [in Ukrainian], Luts. Nats. Tekh. Univer., Kyiv–Luts’k (2010), p. 232.
16. V. V. Skorokhod, *Rheological Fundamentals of the Sintering* [in Russian], Naukova Dumka, Kiev (1972), p. 151.
17. D. A. Konyok, K. V. Voitsekhovskiy, Yu. M. Pleskachevskii, and S. V. Shyl’ko, “Materials with negative Poisson’s ratio,” *Mekh. Kompoz. Mater. Konstr.*, **10**, No. 1, 35–69 (2004).